Potential for Torque Density Maximization of HTS Induction/Synchronous Motor by Use of Superconducting Reluctance Torque

Potential for Torque Density Maximization of HTS Induction/Synchronous Motor by Use of Superconducting Reluctance Torque

Tatsuo Nishimura, Taketsune Nakamura, Quan Li, Naoyuki Amemiya, and Yoshitaka Itoh

***Abstract*—We try to realize the ultimate maximization of torque density in a high-temperature superconducting induction/synchronous motor (HTS-ISM) for transportation equipment. Although the basic structure of the HTS-ISM is almost the same as that of the conventional squirrel-cage induction motor, it can rotate at high-efficiency synchronous speed by the use of superconducting (zero resistance) rotor windings. It has been also shown that torque density can be enormously enhanced at such synchronous rotation mode. In this study, in order to further enhance such torque density, a rectangular superconducting bulk shield is installed in the rotor core. First, we clarified the effectiveness of the HTS bulk based on the analysis and the experiment. Moreover, we succeeded in obtaining no-load and load curves for the speed range from 300 to 1800 r/min.**

***Index Terms*—Bulk, high-temperature superconducting (HTS), induction/synchronous machine (ISM), reluctance torque, shield.**

I. Introduction

OUR research group has been developing the so-called high-temperature superconducting induction/synchronous machine (HTS-ISM) for transportation equipment, such as electric trains, electric buses, and electric vehicles [1], [2]. The basic structure of our machine is the same as that of the conventional squirrel-cage induction motor, and excellent characteristics such as high-efficiency synchronous rotation can be realized by the use of HTS windings [3]–[6]. Followed by the fundamental study [3]–[6], high torque density more than at least ten times larger than that realized by the conventional (normal conducting) motor has been succeeded directly through the experiment [7]. For example, in [7], the HTS squirrel-cage rotor windings are fabricated by the use of the commercial rotor core (stator: conventional copper windings; original rated slip torque: 7.9 Nm), and then, such motor can generate "synchronous torque" more than 80 Nm at 77 K. Based upon the aforementioned success, a 20-kW class prototype motor has recently been developed and then succeeded in testing [1], [2].

Manuscript received July 17, 2013; accepted September 12, 2013. Date of publication September 24, 2013; date of current version October 11, 2013. This work was supported in part by the Grant-in-Aid for Scientific Research (No. 23656199), Japan.

T. Nishimura, T. Nakamura, Q. Li, and N. Amemiya are with Kyoto University, Kyoto 615-8510, Japan (e-mail: tk_naka@kuee.kyoto-u.ac.jp).

Y. Itoh is with IMRA Material R&D Company, Ltd., Kariya 448-0032, Japan.

Color versions of one or more of the figures in this paper are available online at http://ieeexplore.ieee.org.

Digital Object Identifier 10.1109/TASC.2013.2283238

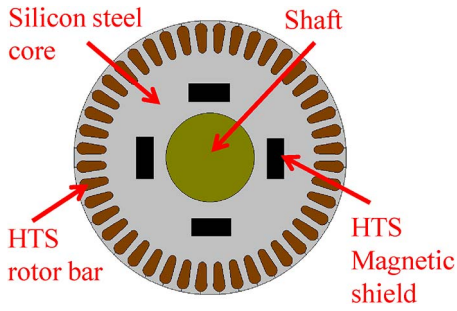

Fig. 1. Schematic diagram of the proposed cross section of HTS rotor.

One of the most important targets for the abovementioned R&D project is the maximization of its torque density. That is, so-called transmission gears for the transportation equipment, which have typically heavy weight and generate losses, can be removed if the motor can generate adequate torque for traction.

In this paper, we try to enhance the torque density of the motor for traction force maximization by the use of the HTS reluctance torque. The magnet torque is realized by means of HTS squirrel-cage windings, and the reluctance torque is generated by means of the HTS shield bulk. Electromagnetic field analysis and experimental results are reported and discussed.

II. Basic Mechanism of Torque Density Enhancement with Aid of HTS Reluctance Torque

The basic structure of the original HTS motor is the squirrel-cage-type induction motor. The detailed structure and characteristics of such motor is described in [3]–[6]. In this study, HTS reluctance torque is further added to the abovementioned induction/synchronous torque (hereafter, stated as magnet torque). Fig. 1 illustrates the schematic diagram of the cross section of the proposed rotor. HTS squirrel-cage windings are installed in the slots, which are located at the outer parts of the rotor core. The HTS magnetic shield bodies (4 in this figure) are also installed in the slots. Fig. 2 shows the conceptual explanation of the maximum torque for different rotational speed. As shown in the figure, there are roughly two kinds of operation modes for the drive motor, i.e., constant torque operation mode at low speed and constant power operation mode at high speed. Generally speaking, the magnetic saturation is not occurred at the steady state, i.e., light load condition. In this region, the magnetic flux lines avoid the HTS shield bulk, and then such bulks do not influence the magnetic circuit. At high torque operation region such as starting, however, the rotor core is

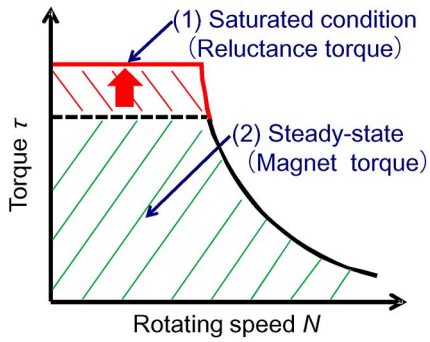

Fig. 2. Conceptual explanation of torque enhancement by using HTS reluctance torque in torque (τ) versus rotating speed (N) plane.

largely been saturated, and the relative permeability of the core decreases correspondingly. Furthermore, the influence of the HTS shield bulk on the magnetic circuit in the rotor will appear in order to generate the reluctance torque at this condition. In other words, the abovementioned HTS reluctance torque is automatically generated by sensing the magnetic condition of the rotor core. It is commonly said that the reluctance torque will decrease the power factor, and this occurs the enlargement of the reactive current. Hence, the magnet torque should only be utilized for the steady-state (medium or light torque) operation mode. At starting, however, high torque is more important than efficiency.

III. Electromagnetic Field Analysis

In order to verify the abovementioned idea, electromagnetic field analysis is carried out. Fig. 1 is modeled for 2-D finite-element analysis (FEA). A normal conducting (copper) stator (three-phase, four-pole, distributed windings, star connection) is considered, and the rotor windings are made of HTS tapes. The air-gap length between the stator and the rotor is 0.3 mm. At present, the analysis is only available for the static condition of the rotor due to the difficulty in the characterization of the HTS.

Fig. 3 shows the examples of analysis results of magnetic flux density contours. As can be seen in Fig. 3(a), clear four magnetic poles are formed at the steady (no saturation) mode (air-gap magnetic flux density: 0.4 T). On the other hand, when the rotor core is in the starting (saturation) mode (1.1 T), doubled magnetic poles, i.e., 8, further add to the four magnetic poles. This shows one of the evidences for the saturation mode reluctance torque. In other words, the reluctance torque is autonomously generated with the aid of the magnetic condition of the rotor core.

Fig. 4 shows the schematic diagram of the magnet torque, the reluctance torque, and the total torque waveforms. Unfortunately, the torque value cannot be quantitatively obtained based on the present analysis, and be our future work.

IV. Fabrication and Rotation Test

A. Fabrication

Based on the analysis results, we try to fabricate the HTS-ISM with an HTS shield body. Fig. 5(a) shows a photograph

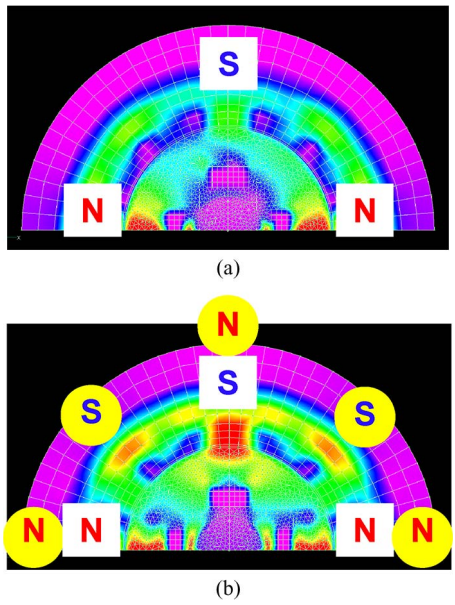

Fig. 3. Analysis result of magnetic flux density contours of HTS rotor at (a) unsaturated and (b) saturated conditions. (a) Unsaturated (air-gap magnetic flux density: 0.4 T). (b) Saturated (air-gap magnetic flux density: 1.1 T).

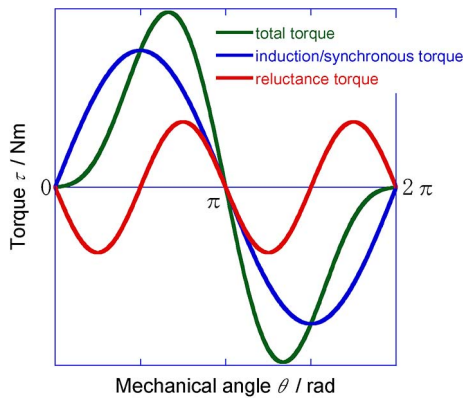

Fig. 4. Schematic diagram of the magnet torque, reluctance torque, and total torque waveforms.

of the Gd-system shield bulk, and the completed HTS rotor is shown in Fig. 5(b). The HTS squirrel-cage windings are made of DI-BSCCO tapes (critical currents at 77 K are 72 A for rotor bars and 166 A for end rings). Five pieces of the DI-BSCCO tapes are stacked together for one rotor bar (total critical current for one rotor bar: 360 A), and then, such rotor bars are installed in a total of 44 slots of the rotor core. After that,

DI-BSCCO end rings are wound by means of the solder. Then, infinitesimal contact resistance is included in the cage windings, even such windings are in the superconducting state.

After completion of the HTS cage windings, we further insert the HTS shield bulk. In this study, two pieces of square-shaped Gd bulks (width: 10 mm; height: 5.0 mm; length: 45 mm) are located in series for one shield body. These bulks are set with the use of the epoxy resin.

B. Experimental Setup

The fabricated rotor is coupled with the conventional (copper) stator (three-phase, four-pole) and then installed in the metal cryostat. Fig. 6 shows the experimental bed. The rotor

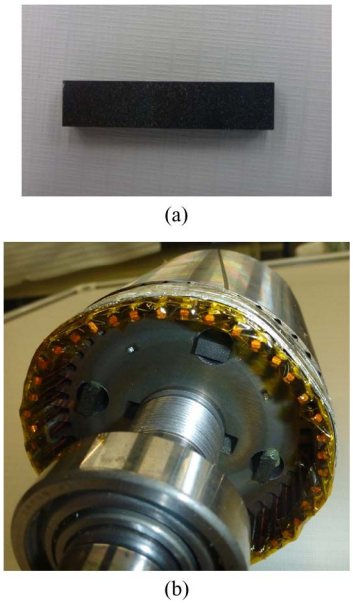

(a)

(b)

Fig. 5. Photograph of fabricated HTS rotor. (a) Gd-system shield bulk. (b) Completed rotor.

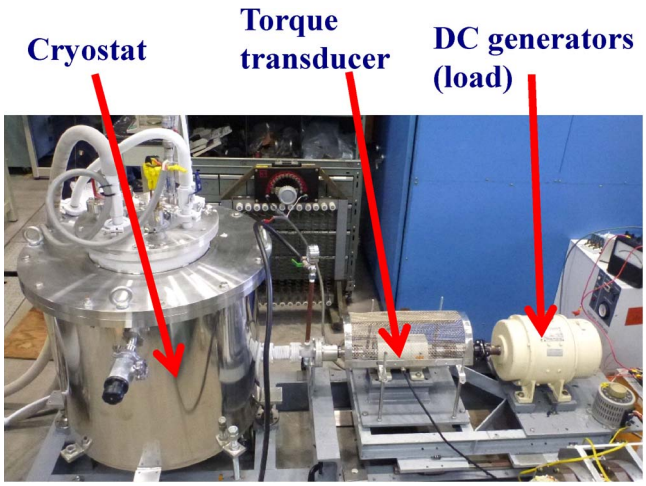

Fig. 6. Photograph of the experimental bed.

shaft of the fabricated HTS motor is connected with that of the load generator by means of the coupling and the magnetic fluid seal. In order to avoid the freeze of the seal, liquid nitrogen going out along the shaft is pushed back by using warm nitrogen gas. A torque transducer is also installed in between the fabricated motor and the load generator.

C. Temperature Dependence of No-Load Characteristics

First, we carried out a no-load test as a function of operation temperature. That is, the HTS-ISM is first pulled in the synchronism (600 r/min) without load at 77 K (in LN_2). Then, the no-load rotation tests are carried out for keeping the magnetomotive force for increasing the process of the operation temperature. This is for the verification of the functionality of both the HTS squirrel-cage windings and the HTS shield bulk on the rotating performance.

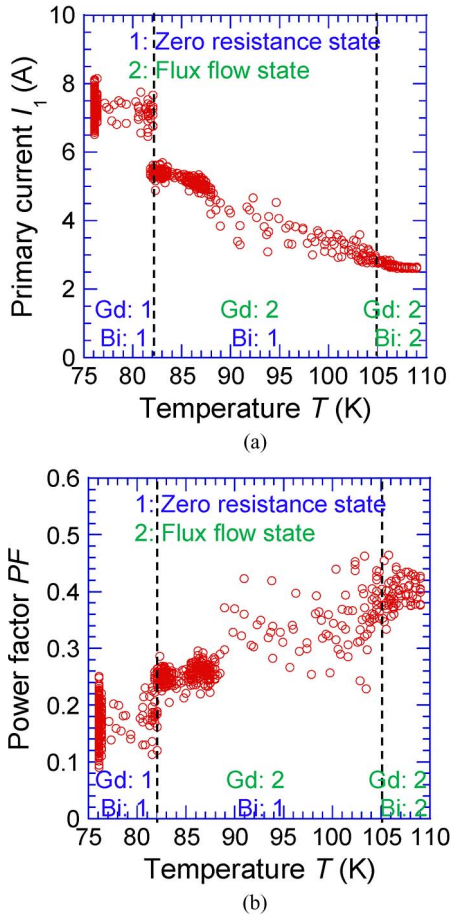

Fig. 7. Experimental results of no-load characteristics at the warm-up process (rotational speed: 600 r/min). (a) Primary current. (b) Power factor.

Fig. 7 shows the tested results for the pumping-out process of liquid nitrogen from the cryostat (warm-up process). The temperature sensor is attached at the outer surface of the stator blanket. Therefore, the temperature of this sensor is not always the same as that of the HTS rotor. Moreover, the liquid nitrogen naturally evaporates from the cryostat during the rotation test, and then, there is large temperature fluctuation at the motor.

As can be seen in Fig. 7(a), the primary current is dropped down to be the small value at around 82 K, and the corresponding power factor is increased at this temperature. This is because the Gd HTS shield bulk reaches for the irreversibility temperature, and the disappearance of the shielding property of the bulk makes the reactive current low.

When the temperature further increases, the current decreases correspondingly because of the decrement of the critical current of the DI-BSCCO cage windings. Finally, such current is converged to be almost of a constant value. At this temperature, the DI-BSCCO cage windings reach for its irreversibility temperature. From these results, it can be verified that both the DI-BSCCO cage windings and the Gd-system shield bulk would be functioned for the rotational performance.

D. Load Test Characteristics

Next, we perform the load characteristics at 77 K. The fabricated motor is first pulled in to be the synchronous speed,

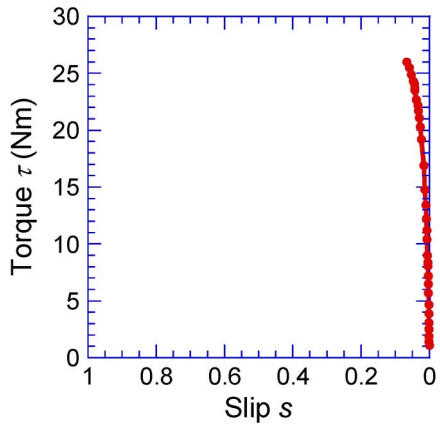

Fig. 8. Example of tested result of torque (τ) versus slip (s) curve at 77 K. The synchronous speed (for the case $s = 0$) is 900 r/min.

and then, the mechanical load is gradually applied to the motor. It should be noted that the presented characteristics in this study are for the steady state.

Fig. 8 shows an example of the load test results at 77 K. The synchronous speed in this test is 900 r/min. As can be seen in the figure, we can clearly observe that the synchronous torque maintains, at least, about 10 Nm. Furthermore, the maximum torque with small slip reaches about 26 Nm.

Actually, this torque curve has been successfully observed just recently, and the detailed analysis will be one of our important future works.

V. Conclusion

In this study, we have proposed and studied the HTS-ISM having HTS reluctance torque at the starting and/or overload condition. The HTS reluctance torque is realized by means of an HTS shield bulk installed in the rotor core. The abovementioned reluctance torque is generated by sensing the magnetic condition of the rotor core, i.e., saturation or no saturation. Our idea is elucidated based on the analysis and the experiment. We are trying to show evidence that the present motor can realize ultimate torque density at starting operation mode.

Acknowledgment

The authors would like to thank Mr. H. Kitano and Mr. S. Misawa from the Department of Electrical Engineering, Graduate School of Engineering, Kyoto University, Kyoto, Japan, for their valuable discussions.

References

[1] D. Sekiguchi, T. Nakamura, S. Misawa, H. Kitano, T. Matsuo, N. Amemiya, Y. Itoh, M. Yoshikawa, T. Terazawa, K. Osamura, Y. Ohashi, and N. Okumura, "Trial test of fully HTS induction/synchronous machine for next generation electric vehicle," *IEEE Trans. Appl. Supercond.*, vol. 22, no. 3, p. 5200904, Jun. 2012.

[2] Q. Li, T. Nakamura, H. Shimura, T. Nishimura, H. Kitano, S. Misawa, N. Amemiya, Y. Itoh, M. Yoshikawa, T. Terazawa, N. Okumura, M. Furuse, and S. Fukui, "Strategy and progress of fully superconducting induction/synchronous motors for environmental-friendly electric vehicles," presented at the 23rd Int. Conf. Magnet Technol., Boston, MA, USA, Jul. 2013, Paper 2OrBA-04.

[3] G. Morita, T. Nakamura, and I. Muta, "Theoretical analysis of a YBCO squirrel-cage type induction motor based on an equivalent circuit," *Supercond. Sci. Technol.*, vol. 19, no. 6, pp. 473–478, Jun. 2006.

[4] T. Nakamura, Y. Ogama, H. Miyake, K. Nagao, and T. Nishimura, "Novel rotating characteristics of a squirrel-cage-type HTS induction/synchronous motor," *Supercond. Sci. Technol.*, vol. 20, no. 10, pp. 911–918, Oct. 2007.

[5] K. Nagao, T. Nakamura, T. Nishimura, Y. Ogama, N. Kashima, S. Nagaya, K. Suzuki, T. Izumi, and Y. Shiohara, "Development and fundamental characteristics of a YBCO superconducting induction/synchronous motor operated in liquid nitrogen," *Supercond. Sci. Technol.*, vol. 21, no. 1, p. 015022, Jan. 2008.

[6] T. Nakamura, K. Nagao, T. Nishimura, Y. Ogama, M. Kawamoto, T. Okazaki, N. Ayai, and H. Oyama, "The direct relationship between output power and current carrying capability of rotor bars in HTS induction/synchronous motor with the use of DI-BSCCO tapes," *Supercond. Sci. Technol.*, vol. 21, no. 8, p. 085006, Aug. 2008.

[7] T. Nakamura, K. Matsumura, T. Nishimura, K. Nagao, Y. Yamada, N. Amemiya, Y. Itoh, T. Terazawa, and K. Osamura, "A high temperature superconducting induction/synchronous motor with a ten-fold improvement in torque density," *Supercond. Sci. Technol.*, vol. 24, no. 1, p. 015014, Jan. 2011.